Wind and Structures, *Vol. 20, No. 6 (2015) 751-761*
DOI: http://dx.doi.org/10.12989/was.2015.20.6.751

Layout optimization for multi-platform offshore wind farm composed of spar-type floating wind turbines

E.H. Choi, J.R. Cho* and O.K. Lim

School of Mechanical Engineering, Pusan National University, Busan 609-735, Korea

(Received October 18, 2014, Revised April 3, 2015, Accepted April 6, 2015)

Abstract. A multi-platform offshore wind farm is receiving the worldwide attention for the sake of maximizing the wind power capacity and the dynamic stability at sea. But, its wind power efficiency is inherently affected by the interference of wake disturbed by the rotating blades, so its layout should be appropriately designed to minimize such wake interference. In this context, the purpose of this paper is to introduce a layout optimization for multi-platform offshore wind farm consisted of $2.5MW$ spar-type floating wind turbines. The layout is characterized by the arrangement type of wind turbines, the spacing between wind turbines and the orientation of wind farm to the wind direction, but the current study is concerned with the spacing for a square-type wind farm oriented with the specific angle. The design variable and the objective function are defined by the platform length and the total material volume of the wind farm. The maximum torque loss and overlapping section area are taken as the constraints, and their meta-models expressed in terms of the design variable are approximated using the existing experimental data and the geometry interpretation of wake flow.

Keywords: layout optimization; multi-platform offshore wind farm; wind turbine spacing; torque loss; overlapping section area; response surface method (RSM)

1. Introduction

Wind turbines for extracting the renewable energy from wind were initially designed to be installed on land, and those showed the rapid increase in both the total number of installations and the maximum wind power capacity to some extent (Hansen and Hansen 2007). However, this rapid increase has been declined owing to several obstacles such as the substantial environmental impact on people living around the wind turbines and the limitation of being large-capacity. Such a restrictive situation naturally turned the attention to the offshore sites, a less restrictive place capable of providing more stable wind of high quality. In general, offshore wind turbines are classified into two categories, fixed- and floating-type depending on how the wind turbine is supported, and the floating-type is divided into three kinds; barge, tension leg (TLP) and spar according to the type of floating substructure (Lee 2008, Jonkman 2009, Bae and Kim 2011). The current study is concerned with the spar-type floating offshore wind turbine.

Differing from the fixed-type, the floating-type is still under the on-site proving experiment

*Corresponding author, Professor, E-mail: jrcho@pusan.ac.kr

http://www.techno-press.org/?journal=was&subpage=8 ISSN: 1226-6116 (Print), 1598-6225 (Online)

stage because several core technologies are not fully settled down (Karimirad *et al*. 2011), particularly the securing of dynamic stability to irregular wind, wave and current loads. The dynamic stability of floating offshore wind turbine is meant by the station keeping at sea and the suppression of rotational oscillation (Tong 1998). The station keeping has been traditionally secured by mooring lines, while the rotational oscillation has been suppressed by adjusting the center positions of gravity and buoyancy and the fairlead location for mooring lines (Jeon *et al.* 2013). Meanwhile, the floating offshore wind farm has been studied worldwide in order to maximize the wind power capacity and the dynamic stability (Tong 1998, Mosetti *et al*. 1994, Zhixin *et al*. 2009). Offshore wind farms are basically classified into two categories, a simple grouping of separate wind turbines within the specific region and the assembling of wind turbines all together into a multi-platform structure. The former is adopted for the fixed-type offshore wind turbines, while the latter is for the floating-type offshore wind turbines thanks to its effectiveness in suppressing the rotational oscillation (Kosugi *et al.* 2002).

Regardless of the type, a common consideration in the design of wind farm is the minimization of interference of disturbed wake among the wind turbines. The interaction between undisturbed wind and the rotating blades causes turbulent wake of relatively reduced wind velocity, so that the power capacity of wind turbines at downstream could be significantly affected by the disturbed wake (Whale *et al*. 2000, Vermeer *et al*. 2003). Whether the interference of wake occurs or not and its intensity are dependent of the spacing between wind turbines, the way of wind turbine arrangement and the wind farm orientation to the wind direction (Johnson and Thomas 2009, Adaramola and Krogstad 2011). Such an interference could be avoided by making the spacing large enough, but the assembling and maintenance cost should be considered, particularly in the design of multi-platform wind farm.

In this context, this paper introduces a layout optimization for multi-platform offshore wind farm composed of spar-type floating offshore wind turbines. A square-type wind farm arrangement composed of nine wind turbines is considered by defining the platform length and total material volume as the design variable and objective function, respectively. The meta-models of the maximum shaft torque loss and overlapping section which are set by the constraints are approximated in terms of the design variable using the existing experimental data and the geometric interpretation of wake flow, respectively.

2. Floating offshore wind farm

2.1 Spar-type floating offshore wind turbine

Fig. 1(a) shows a typical spar-type floating offshore wind turbine supported by the buoyancy force produced by the hollow cylindrical floating substructure. The wind tower supporting the upper part and the floating substructure is assembled such that the assembling interface is positioned just below the water free surface. Differing from the fixed-type, the floating-type may exhibit the remarkably unstable dynamic response in the horizontal, vertical and rotational directions when it is subject to unstable wind, wave and current loads (Faltinsen 1990, Waris and Ishihara 2012). The dynamics stability of the floating wind turbine is usually meant by the station keeping at sea and the stable rotational oscillation. The station keeping is maintained by thee mooring cables connected to the substructure, while the rotational oscillation is suppressed by adjusting the center positions of mass and buoyancy and the connection position of mooring cables.

It could be suppressed further when passive tuned liquid damper (TLD) or/and active control using water ballast are employed (Lee *et al.* 2006, Colwell and Basu 2009). Regarding the dynamic displacement of wind turbine, only surge and sway displacements are counteracted by the mooring lines when a catenary mooring system is adopted while the displacements in all DOFs are counteracted by tension lines if a TLP system is adopted (Lefebvre and Collu 2012).

Referring to Fig. 1(a), the rigid body dynamic motion of floating-type wind turbine is expressed in terms of three translational motions, surge, sway and heave and three rigid rotational motions, pitch, roll and yaw. These six rigid body motions are coupled to some extent, and the pitch, roll, surge, sway and heave motions are considered as important factors in the dynamic stability evaluation of floating-type wind turbine. Surge, sway and heave motions influence the station keeping of platform while pitch and roll motions affect the rotational oscillation of platform. The dynamic stability may not only influence the structural safety of the whole wind turbine but also degrade the wind power efficiency, so that it is now widely investigated by making use of the numerical simulation or/and the scale-model experiment in wave tanks equipped with the wind generation system (Utsunomiya *et al.* 2010, Goopee *et al*. 2012, Bae and Kim 2013, Dinh *et al*. 2013). Meanwhile, the construction of low-cost wind farm by combining a number of floating wind turbines is also intensively in consideration not only for securing the dynamic stability but also for increasing the wind power capacity (Tong 1998, Lee 2012). Fig. 1(b) represents the major dimensions of a 2.5*MW*-class spar floating wind turbine under consideration in the current study.

2.2 Concept of floating offshore wind farm

Fig. 2(a) shows a multi-platform having four floating offshore wind turbines that becomes a base module for the floating offshore wind farm. In other words, a floating offshore wind farm could be constructed by combining the desired number of base modules and the overall configuration and dimensions are determined by the total number of base modules and the way of arrangement. A base module is composed of wind turbines, platforms, substructures and mooring lines. The platforms combine wind turbines at regular spacing and provide the working space for assembling and maintenance, while a number of mooring lines are used for the station keeping at sea and the substructures produce the buoyancy force to support the whole base module. A substructure consists of several cylindrical blocks as represented in Fig. 2(b); a rotatable block at the top for rotating the wind turbine according to the wind direction, a ballast block at the bottom for damping the rotational oscillation of wind turbines owing to the wind and wave excitations, and the remaining floating blocks for producing the buoyancy force.

One of the major concerns in the design of offshore wind farm is the layout of wind turbines, where the term layout means the spacing between wind turbines and the orientation of wind farm with respect to the wind direction. It is of course because both factors directly influence the wind power efficiency. The interaction between undisturbed wind flow and the rotating blades causes the unsteady wake (Johnson and Thomas 2009), which results in the distributed downstream wind of remarkably reduced wind velocity. Thus, the wind turbines behind up-front ones may be within the influence of disturbed wake unless the spacing is large enough. The influence intensity of unsteady wake on the wind turbines at downstream is dependent of the orientation of wind farm because the lateral distance between the wake flow path and the wind turbine at downstream is affected by the orientation (Whale *et al*. 2000). It will be explained more in detail in the next section.

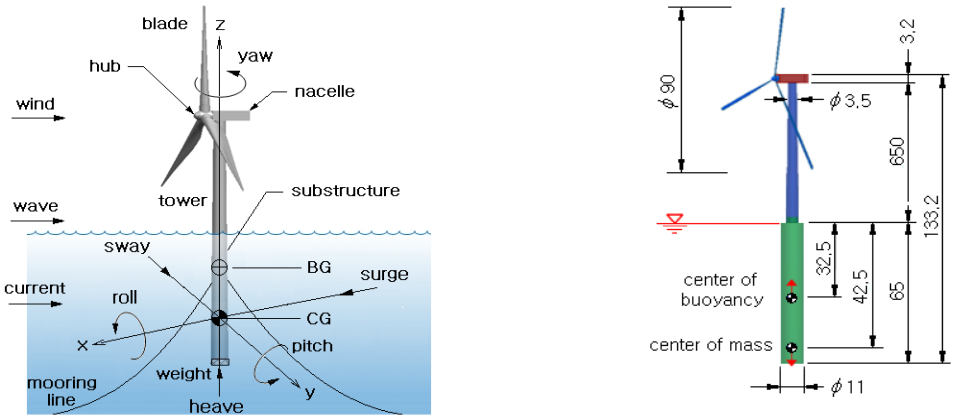

Fig. 1 (a) Spar-type floating offshore wind turbine: (a) major components and 6-DOF rigid body motions (CB: center of buoyancy, CG: center of gravity), (b) major dimensions (unit: *m*)

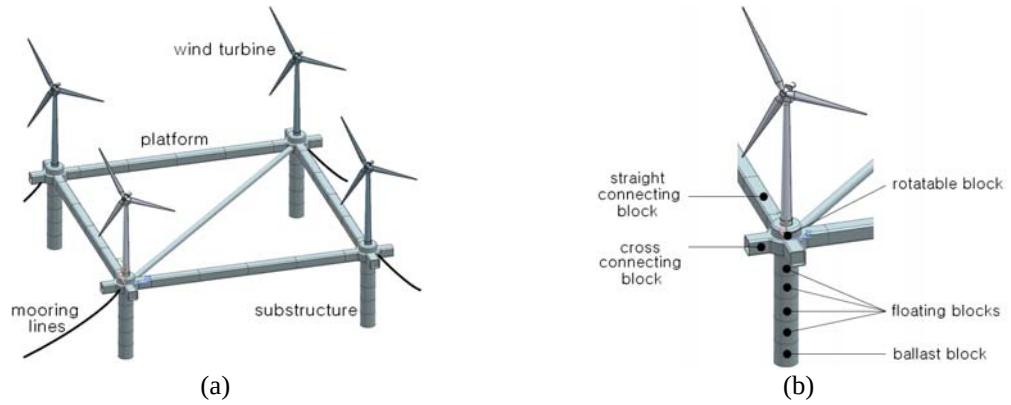

Fig. 2 (a) A base multi-platform composed of four wind turbines, (b) block-type assembling

3. Layout optimization of floating offshore wind farm

3.1 Influence of unsteady wake at downstream

The passing of laminar flow through fixed or moving objects is always accompanied by turbulent wake of relatively reduced flow velocity. Since the wind power efficiency is definitely influenced by the wind flow quality, the interference of disturbed wake to the wind turbines at downstream should be considered in the design of wind farm. Fig. 3(a) represents the disturbed wake flow behind the rotating wind blades, where D stands for the diameter of rotor blades. The flow profile was obtained by CFD simulation for which the diameter D and the velocity V of up-front uniform flow were set by $90m$ and $10m/sec$, respectively. The wake flow shows uniform expansion in the radial direction to a certain distance from the rotating blades, but the flow diameter is kept almost constant thereafter. It has been reported from the wake model

simulation (Barthelmie *et al*. 2006, Marmidis *et al*. 2008) that both the expansion distance and the expanded diameter are a function of rotor diameter D. The 3-D flow geometry of disturbed wind behind the rotating blades is required for the influence analysis of wake on the wind turbines at downstream. It is simplified as a conical and cylindrical domain as shown in Fig. 3(b), where the expansion distance and the expanded diameter are $2.25D$ and $5.0D$, respectively. The flow configuration and two parameters will be used for the geometry interpretation of wake interference.

Fig. 4(a) schematically represents the influence of wake in case of a square wind farm composed of nine wind turbines, where the dotted circles indicate the wind turbines which may be under the interference of wake caused by up-front rotor blades. The distances L_t and L_o indicate the spacing between wind turbines in the directions parallel and normal to the wind flow, respectively. The number and location of wind turbines at downstream which are under the influence of disturbed wake are dependent of the wind velocity and the spacing between wind turbines as well as the way of wind turbine arrangement in the wind farm and the orientation of wind farm to the wind direction. In the current study, square-type wind farms having equal spacing are considered, in which the total number of wind turbines becomes N^2 with N being the number of wind turbines in each direction.

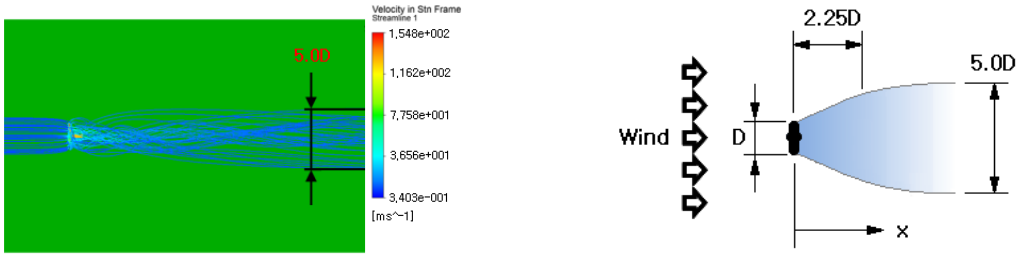

(a) (b)

Fig. 3 wake behind the rotating blades: (a) CFD simulation, (b) flow configuration and dimensions

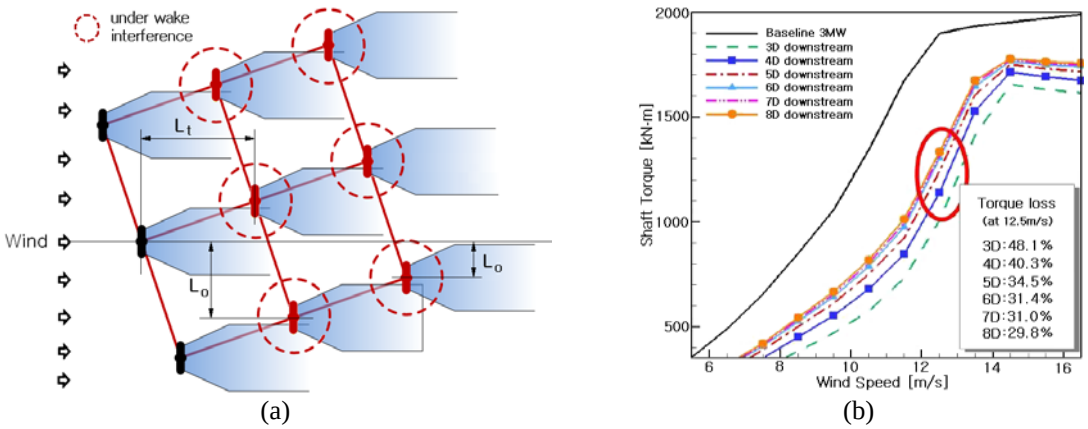

(a) (b)

Fig. 4 (a) Wake interference in case of a square wind farm, (b) variation of torque loss to the wind speed at different downstreams (Lee 2012)

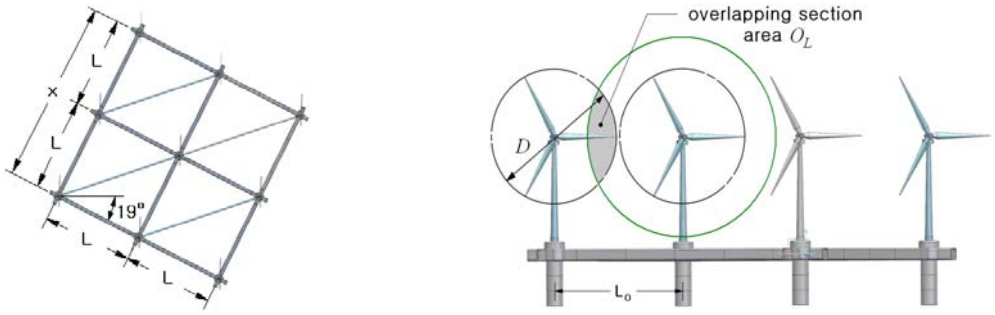

(a) (b)

Fig. 5 A square wind farm model: (a) configuration and the design variable ($\theta = 19^\circ$), (b) lateral interference of wake flow

The influence of distributed wake results in the torque loss of input shaft of wind turbine because the wind velocity of disturbed wake is relatively slower than the undisturbed far-field wind. Fig. 4(b) represents the variation of shaft torque of a $3MW$ wind turbine which is located behind another $3MW$ wind turbine to the far-field undisturbed wind velocity. The plot was obtained by the on-site proving experiment (Lee 2012) with two $3MW$ wind turbines lined up in the wind direction, and the baseline in the plot indicates the shaft torque measured without an up-front wind turbine. The torque loss caused by the interference of disturbed wake is evaluated with the respect to the baseline, and it monotonically decreases in proportional to the spacing L_t between two wind turbines. It is known that the influence of disturbed wake completely disappears when the spacing is sufficiently large enough.

3.2 Optimization formulation

The wak interference between wind turbines is influeced by the layout pattern, the orientation angle of wind farm and the distance between wind turbines. But, for the illustrative purpose, the layout pattern is assumed to be square and the orientation angle was set by a specific angle for the current study. A square wind farm having the equal spacing shown in Fig. 4(a) which is composed of nine wind turbines is taken for the layout optimization in the current study. However, the optimization methodology introduced in this paper could be applied to other wind farms composed of different numbers of wind turbines, even for different arrangements, without loss of generality. A square-type wind farm is represented in Fig. 5(a), where the orientation angle θ is set by 19^o while the platform length L is to be tailored. The angle is chosen by a preliminary geometry interpretation such that the interference of wake at downstream becomes to be minimum. The wind direction at the far-off sea is in general kept constant, differing from the wind condition on land, so the wind farm is usually to be oriented based on the geometry interpretation between the wind farm and the main wind direction at the installation location. Fig. 5(b) represents the overlapping section area O_L defined by the relative section area to the circular area of wind turbine blades which is affected by the disturbed wake caused by up-front wind turbine. Differing from the shaft torque loss which estimates the wake interference between two up-front and downstream wind

turbines aligned almost in the wind direction, the overlapping section area estimates the lateral interference of wake caused by the up-front wind turbines which are not in the same row, as represented in Fig. 4(a).

We define the design variable x and the objective function $F(x)$ by two times of the platform length L and the total material volume of the wind farm including nine wind turbines. Thus, the objective function becomes the total material volume of platforms, diagonal connecting bars and wind turbines. Then, the optimization problem is formulated as

$$\underset{x}{\text{Minimize}}\ F(x),\quad x = 2 \times L \tag{1}$$

$$\text{subject to}\quad max\, T_L(x) \le T_L(6D) \tag{2}$$

$$max\, O_L(x) \le O_L(3D) \tag{3}$$

with $T_L(x)$ and $O_L(x)$ being the shaft torque loss and the overlapping section area, respectively. The term *max* is used to indicate the maximum value among nine wind turbines in the square wind farm under consideration. Two constraints are defined; the shaft torque loss for the wake interference at downstream and the overlapping section area for the lateral wake interference. According to the design guideline by Bailey *et al.* (2012), the shaft torque loss $T_L(x)$ is constrained to be less than 31.4% corresponding to one at $6D$ downstream as shown in Fig. 4(b), while the overlapping section area $O_L(x)$ is set smaller than one at $3D$ downstream. Note that it is found from the geometry interpretation that O_L becomes zero when the projected platform length L_o is larger than $3D$.

4. Numerical results

The response surfaces (i.e., meta-models) for the objective function $F(x)$ and two constraints $T_L(x)$ and $O_L(x)$ are constructed by a three-level design of experiments for which the design variable is set by $800, 1{,}000$ and $1{,}200m$, respectively. The wind farm CAD models for each design level are firstly constructed to calculate the total material volumes and the overlapping section areas. The meta- models for $F(x)$ and $O_L(x)$ are constructed by linearly and quadratically interpolating the total material volumes and the overlapping exction areas at three design levels, respectively. Meanwhile, the torque losses given in Fig. 4(b) are firstly interpolated using a forth- order polynomial in terms of D in order to construct a response surface of $T_L(x)$. Next, the platform lengths projected in the wind direction (i.e., L_t in Fig. 4(a)) at each design level are converted to the values with respect to the rotor diameter $D = 90m$, and the torque losses at three design levels are calculated by substituting the converted platform lengths into the forth-order approximation of torque loss. The linear interpolation of the torque losses at three design levels leads to a response of torque loss $T_L(x)$. The approximated meta-models are as follows

$$F(x) = 10{,}999.0x + 39{,}310.0 \tag{4}$$

$$T_L(x) = -18.09x + 200.0 \tag{5}$$

$$O_L(x) = 1.242x^2 - 22.568x + 123.110 \tag{6}$$

where the units are m^3 for $F(x)$ while % for $T_L(x)$ and $O_L(x)$. The accuracy of three metal models was confirmed such that the coefficients of determinant R^2 are 1.0 for three models. Referring to Fig. 2(a), the cross sections of platforms and connecting bar having the same thickness of $0.5m$ are hollow square and hollow circle with the outer width and diameter are 8.0 and $2.5m$, respectively. Meanwhile, the total material volume of nine wind turbines except for the platforms and connecting bars is $39{,}310m^3$.

The optimization was carried out by the generalized reduced gradient algorithm (Abadie *et al.* 1996) for the nonlinear optimization problem with nonlinear constraints, where the initial design variable x_{ini} and the convergence criterion ε_T are set by $10\times10^3 m$ and 1.0×10^{-4}, respectively. The optimization iteration terminates in three iterations, and Fig. 6 represents the detailed iteration histories of the objective function $F(x)$ and the design variable x. The optimization results are given in Table 1, together with the comparison of other two wind farm layouts, where the values in parenthesis indicate the relative change with respect to the initial layout. The optimum design variable is $11.06\times10^3 m$ so that the actual platform length parallel to the wind flow becomes to be $6.08D$ as represented in Fig. 7(a). In other words, the spacing between two wind turbines in the direction of wind is 6.08 times of the circle of rotor blades. The optimum layout leads to the increase of the platform length and the total material volume by 11.6 % and 6.2% respectively, when compared with the initial layout. But, the maximum torque loss T_L has been decreased by 14.9% and the maximum overlapping section has been completely disappeared.

The initial and 8×8 layouts lead to the maximum torque loss less than 31.4% but those suffer from the remarkable lateral wake interference having the maximum O_L greater than 20%. On the other hand, the 12×12 layout satisfies the constraints on the maximum torque loss and overlapping section area, but it is not desirable because the volume increase is more severe than the torque loss reduction. But, if the trade-off among the total material volume, the maximum torque loss and the maximum overlapping section area is desired by the designer's decision making, the current optimization problem could be converted to a multi-objective optimization problem by introducing the weighting factors (Cho *et al.* 2002). Fig. 7(b) shows the arrangement of nine wind turbines when viewed in the direction of wind. One can realize that the wake interference is caused mostly by the left four up-front wind turbines

One of major obstacles in commercializing the floating offshore wind turbine is its low economic efficiency which is evaluated in terms of the production and maintenance cost per unit power generation in megawatt. The concept of wind farm by assembling a number of wind turbines using a multi-platform was introduced to overcome this obstacle. However, it still remains the wake interference problem between neighboring wind turbines and the production cost of multi-platform. In this context, the numerical example presented in this paper illustrates that the layout optimization technique could be usefully applied to design the wind farm which minimizes the wake interference and the production cost at the same time. In addition, the present method could be extended to deal with the layout optimization problem with more than one design variable and objective function.

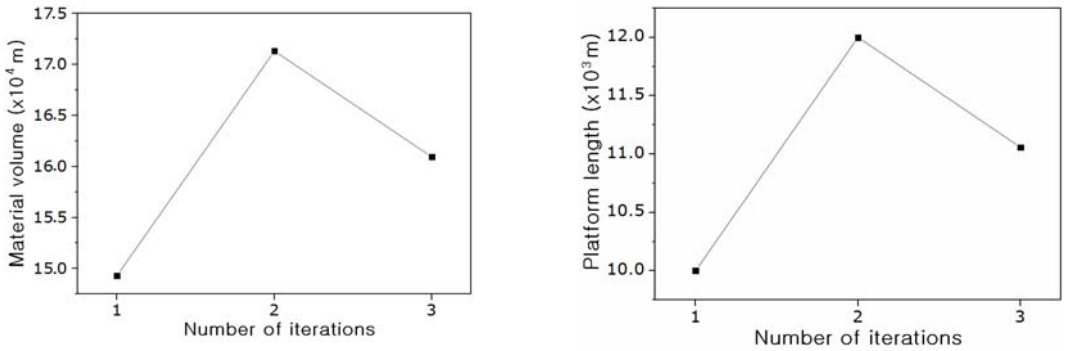

(a) (b)

Fig. 6 Iteration histories: (a) objective function, (b) design variable

Table 1 Optimum layout and the comparison with three wind farm layouts

Items	Platform layouts			
	8×8	Initial 10×10	Optimum	12×12
Design variable $x\left(\times10^3 m\right)$	8.0	10.0	11.06 (+11.6%)	12.0
Platform length parallel to the flow direction L_t	$4.39D$	$5.49D$	$6.08D$	$6.59D$
Objective function $F\left(\times10^4\ m^3\right)$	12.73	15.15	16.09 (+6.2%)	17.13
Maximum torque loss $T_L(\%)$	31.18	25.45	21.65 (-14.9%)	22.07
Maximum overlapping section area $O_L(\%)$	55.30	20.03	0.0	0.0

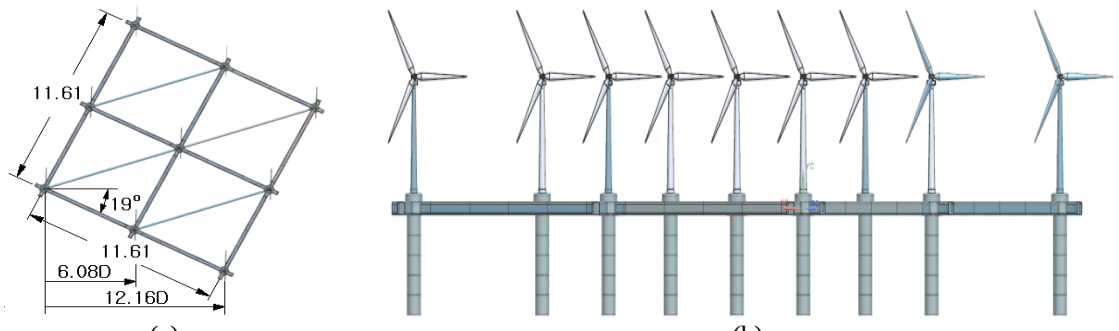

(a) (b)

Fig. **7** Optimum layout of wind farm: (a) basic specifications (unit: $\times10^3 m$, (b) view in the direction of wind

5. Conclusions

The layout optimization of the square-type multi-platform wind farm consisted of spar-type floating offshore wind turbines has been introduced. The optimization problem was formulated by taking the spacing between wind turbines and the total material volume of wind farm as the design variable and the objective function, respectively. The maximum torque loss and overlapping section area were defined as the constraints to reflect the wind power loss caused by the wake interference between wind turbines. The meta-models in terms of the design variable for both constraints were approximated using the on-site proving experimental data and the geometric interpretation of 3-D CAD models of wind farm. The proposed method successfully led to an optimum layout for the square-type wind farm consisted of nine $2.5MW$ wind turbines having the platform length equal to $11.06\times10^3 m$. The total material volume increased by 6.2% when compared to the initial layout having the platform length of $10.0\times10^3 m$, but the maximum torque loss remarkably reduced by 14.9% and the maximum overlapping section area disappeared completely.

Acknowledgements

This work was supported by the New & Renewable Energy of the Korea Institute of Energy Technology Evaluation and Planning (KETEP) grant funded by the Korea government Ministry of Knowledge Economy (No. 2011T100100320).

References

Abadie, J. and Carpentier, J. (1996), "Généralisation de la Méthode du Gradient Réduit Wolfe au Cas de Constraints Nonlieéaires", *Proceedings of the IFORS Congress*, Cambridge, Massachusetts.

Adaramola, M.S. and Krogstad, P.A. (2011), "Experimental investigation of wake effects on wind turbine performance", *Renew. Energ.*, **36**(8), 2078-2086.

Bae, Y.H. and Kim, M.H. (2011), "Rotor-floater-mooring coupled dynamic analysis of mono-column-TLP-type FOWT(Floating Offshore Wind Turbine)", *Ocean Syst. Eng.*, **1**(1), 95-111.

Bae, Y.H. and Kim, M.H. (2013), "Influence of failed blade-pitch-control system to FOWT by aero-elastic-control-floater-mooring coupled dynamic analysis", *Ocean Syst. Eng.*, **3**(4), 295-307.

Bailey, B.H., Beaucage, P., Bernadett, D.W. and Brower, M. (2012), *Wind Resource Assessment: A Practical Guide to Developing a Wind Project*, John Wiley & Sons, New Jersey.

Barthelmie, R.J., Folkerts, L., Larsen, G.C., Rados, K., Pryor, S.C., Frandsen, S.T., Lange, B. and Schepers, G. (2006), "Comparison of wake model simulations with offshore wind turbine wake profiles measured by sodar", *J. Atmos. Ocean.Tech.*, **23**(7), 888-901.

Cho, J.R., Jeong, H.S. and Yoo, W.S. (2002), "Multi-objective optimization of tire carcass contours using a systematic aspiration-level adjustment procedure", *Comput.Mech.*, **29**(6), 498-509.

Colwell, S. and Basu, B. (2009), "Tuned liquid column dampers in offshore wind turbines for structural control", *Eng. Struct.*, **31**, 358-368.

Dinh, V.N., Basu, B. and Nielsen, S.R.K. (2013), "Impact of spar-nacell-blade coupling the edgewise response of loating offshore wind turbines", *Coupled Syst. Mech.*, **2**(3), 231-253.

Faltinsen, O.M. (1990), *Sea Load on Ships and Offshore Structures*, University of Cambridge.

Goopee, A.J., Koo, B.J., Lambrakos, K.F. and Kimball, R.W. (2012), "Model tests for three floating wind

turbine concepts", *Proceedings of the Offshore Technology Conference*, Houston, USA.
Hansen, A.D. and Hansen, L.H. (2007), "Wind turbine concept market penetration over 10 years (1995-2004)", *Wind Energy*, **10**(1), 81-97.
Jeon, S.H., Cho, Y.U., Seo, M.W., Cho, J.R. and Jeong, W.B. (2013), "Dynamic response of floating substructure of spar-type wind turbine with catenary mooring cables", *Ocean Eng*., **72**, 356-364.
Johnson, K.E. and Thomas, N. (2009), "Wind farm control: addressing the aerodynamic interaction among wind turbines", *Proceedings of the 2009 American Control Conference*, St. Louis, MO, USA.
Jonkman, J. (2009), "Dynamics of offshore floating wind turbines-model development and verification", *Wind Energy*, **12**, 459-492.
Karimirad, M., Meissonnier, Q., Gao, Z. and Moan, T. (2011), "Hydroelastic code-to-code comparison for a tension leg spar-type floating wind turbine", *Marine Struct.*, **24**(4), 412-435.
Kosugi, A., Ogata, R., Kamegawa, H., Akutsu, Y. and Kinoshita, T. (2002), "A feasibility study on a floating wind farm off Japan coast", *Proceedings of the 12th (2002) International Offshore and Polar Engineering Conference*, Kitakyushu, Japan.
Lee, H.H., Wong, S.H. and Lee, R.S. (2006), "Response mitigation on the offshore floating platform system with tuned liquid column damper", *Ocean Eng.*, **33**(8-9), 1118-1142.
Lee, S.G. (2012), *Development of Design Optimization Techniques for Wind Farm*, *Technical Report (in Korean)*, Engineering Research Institute, Seoul National University, Korea.
Lee, S.H. (2008), *Dynamic Response Analysis of Spar Buoy Floating Wind Turbine Systems*, Ph.D. Thesis: MIT.
Lefebvre, S. and Collu, M. (2012), "Preliminary design of a floating support structure for a 5MW offshore wind turbine", *Ocean Eng.*, **40**, 15-26.
Marmidis, G., Lazarou, S. and Pyrgioti, E. (2008), "Optimal placement of wind turbines in a wind park using Monte Carlo simulation", *Renew. Energ.*, **33**(7), 1455-1460.
Mosetti, G., Poloni, C. and Diviacco, B. (1994), "Optimization of wind turbine positioning in large windfarms by means of a genetic algorithm", *J. Wind Eng. Ind. Aerod.*, **51**(1), 105-116.
Tong, K.C. (1998), "Technical and economic aspects of a floating offshore wind farm", *J. Wind Eng. Ind. Aerod.*, **74-76**, 399-410.
Utsunomiya, T., Matsukuma, H. and Minoura, S. (2010), "On sea experiment of a hybrid SPAR for floating offshore wind turbine using 1/10 scale model", *Proceedings of the ASME 2010 29th International Conference on Ocean, Offshore and Artic Engineering*, Shanghai, China.
Vermeer, L.J., Sørensen, J.N. and Crespo, A. (2003), "Wind turbine wake aerodynamics", *Prog. Aerosp. Sci.*, **39**(6-7), 467-510.
Waris, M.B. and Ishihara, T. (2012), "Dynamic response analysis of floating offshore wind turbine with different types of heave plates and mooring systems by using a fully nonlinear model", *Coupled Syst. Mech.*, **1**(3), 247-268.
Whale, J., Anderson, C.G., Bareiss, R. and Wagner, S. (2003), "An experimental and numerical study of the vortex structure in the wake of a wind turbine", *J. Wind Eng.*, **84**(1), 1-21.
Zhixin, W., Chuanwen, J., Qian, A. and Chengmin, W. (2009), "The key technology of offshore wind farm and its new development in China", *Renew. Sust. Energy. Rev.*, **13**(1), 216-222.

CC